Islands in locally-forced basin circulations

Sam Potter

1 Abstract

The circulation response of a square basin with an island and localized surface stress curl is discussed. Attempts in a laboratory were unsuccessful due to unforeseen difficulties in applying a localized surface stress curl to a rotating tank experiment. Numerical simulations show that the effect of an island on the circulation of a square basin with localized forcing can for the most part be characterized by Kelvin's circulation theorem. The circulation response is shown to depend on whether the island has vertical or sloped walls.

2 Introduction

2.1 Simple gyre circulations

Stommel (1948) and Munk (1950) ([8, 3]) created a simple theory for understanding the gyre circulations of the oceans. Both of these papers solve for the steady state flow field of a homogeneous small Rossby number ocean forced by a wind stress curl. The equation to consider, from [4]

$$\frac{\partial}{\partial t}\nabla^2\psi + \epsilon J(\psi, \nabla^2\psi) + \frac{\partial \psi}{\partial x} = \text{curl}\boldsymbol{\tau} - \mu\nabla^2\psi + E\nabla^4\psi. \tag{1}$$

Here ψ is the streamfunction and

$$\epsilon = \frac{U}{\beta L^2} = \left(\frac{\delta_I}{L}\right)^2 \tag{2}$$

$$\mu = \frac{r}{\beta L} = \left(\frac{\delta_S}{L}\right) \tag{3}$$

$$E = \frac{\nu}{\beta L^3} = \left(\frac{\delta_M}{L}\right)^3. \tag{4}$$

U and L are the scaling velocity and length, respectively. r is the bottom friction coefficient, ν is viscosity and $\beta = \frac{df}{dy}$ is the meridional gradient of the Coriolis parameter. The first and second terms on the LHS of (1) are the material derivative of the relative vorticity

and the third term is the meridional advection of planetary vorticity. The first term on the RHS of (1) is the curl of the wind stress and the second and third terms are bottom friction and lateral friction, respectively. δ_I, δ_S, δ_M are the inertial, Stommel and Munk boundary layer widths. Since the nondimensional numbers above are functions of these boundary layer widths, the nonlinearity of the system can be framed in terms of δ_I/δ_S or δ_I/δ_M. A larger δ_I/δ_S means the system is more nonlinear. In this report δ_I is calculated as $\delta_I = \sqrt{U_S/\beta} = \sqrt{\text{curl}\tau/\beta^{\mathbf{2}}}$ where $U_S = \text{curl}\tau/\beta$ is the Sverdrup flow.

Considering a steady state and assuming that ϵ, the Rossby number for this system, is small, the first two terms on the left hand side of (1) are dropped. For the Stommel model $\nu := 0$, and vorticity is modified by bottom friction with r^{-1} the frictional timescale. In the Munk model $r := 0$ and lateral viscosity takes the place of bottom friction. The solution streamfunction can be found found by splitting the solution into two parts: a frictionless interior where either viscosity or bottom drag can be ignored and a frictional boundary layer, where length scales are short enough for friction to be important. Following [10] an explicit approximate solution can then be found by asymptotically matching the Sverdrup flow of the geostrophic interior, where $\frac{\partial \psi}{\partial x} = \text{curl}\tau = \mathbf{w_E}$, to the western boundary layer solution where friction is important. For the nondimensional Stommel problem the approximate streamfunction solution with a wind stress of $\boldsymbol{\tau} = (-\cos(\pi y), 0)$ is given by $\psi = \pi(1 - x - e^{x/d})\sin(\pi y)$ (see Figure 1). From (2), $d = \delta_S/L = \mu$ is the nondimensional width of the frictional western boundary layer and is assumed to be much less than one. The solution of the Munk problem is not shown here but exhibits the same basic characteristics as figure 1.

The solution of the Stommel and Munk problems forced with anticyclonic (cyclonic) wind curl exhibit two features: slow anticyclonic (cyclonic) flow in the interior of the ocean and fast northward (southward) flow in the western boundary current. This report will deal with several modifications of this ocean circulation theory. I will be considering how the gyre circulation is changed when (a) the wind forcing is localized, not universal, and (b) there exists an island with or without topography in the basin.

2.2 Gyre circulation with islands

Adding an island to the Stommel-Munk setup creates a multiply connected domain. This allows for the existence of an island circulation, defined as the total transport between the island and the outer basin boundary. When the circulation is in steady state and linear and the bulk of the dissipation takes place on the eastern side of the island, which acts as a western boundary for the sub-basin east of the island, the island transport can be solved

for using the Island Rule of Godfrey [1, 6].

Following Pedlosky et al. (1997) the Island Rule can be derived starting from the horizontal momentum equations for a single homogeneous layer:

$$\frac{\partial \mathbf{u}}{\partial t} + (\zeta + f)\hat{k} \times \mathbf{u} = -\nabla \left(\frac{p}{\rho} + \frac{|\mathbf{u}^2|}{2} \right) + \text{Diss}(\mathbf{u}) + \mathbf{T} \tag{5}$$

where $\mathbf{T}$ is a forcing (e.g. wind stress), Diss($\mathbf{u}$) is dissipation, either bottom friction, lateral friction or both, ζ is relative vorticity, and the first term on the right hand side is the Bernoulli function. The β-plane approximation is made, making $f = f_0 + \beta y$. To determine the island streamfunction it is necessary to integrate around the island, but this creates a problem since the eastern side of the island contains a highly dissipative western boundary. Assuming that the only non-negligible dissipation due to the island occurs on the *eastern* side, the trick of Godfrey is to create a contour that avoids this western boundary (see figure 2). Integrating around a circuit that only sees ocean interior and eastern boundaries allows the Diss($\mathbf{u}$) term to be ignored. Assuming that the flow is linear, in a steady state and is non-divergent (so a streamfunction can be defined) integrating (5) around the contour C defined in figure 2 gives

$$\beta(y_n - y_s)\psi_I = -\oint_C \mathbf{T} \cdot \hat{t} ds, \tag{6}$$

where y_s and y_n are the southernmost and northernmost latitudes of the island, respectively, and ψ_I is the island streamfunction, which is assumed to be zero on the eastern basin boundary and a constant on the island. This relation can be further simplified by defining a Sverdrup streamfunction

$$\beta\psi_S = -\int_x^{x_e} \hat{k} \cdot \nabla \times \mathbf{T} dx'$$

where x_e is the x-coordinate of the eastern basin boundary. Using Stokes Theorem the forcing term in (6) becomes

$$\begin{aligned} \oint_C \mathbf{T} \cdot \hat{t} ds &= \oint_{C_I} \mathbf{T} \cdot \hat{t} ds + \int\int_R \beta \frac{\partial \psi_S}{\partial x} dx dy & (7) \\ &= \oint_{C_I} \mathbf{T} \cdot \hat{t} ds - \beta \int_{y_s}^{y_n} \psi_S(x_+, y) dy, & (8) \end{aligned}$$

Here x_+ is the x-coordinate of the eastern side of the island and C_I is the counter-clockwise circuit around the island. If we assume there is no net tangential force around the island

the first term on the right hand side of (8) drops out and (6) becomes

$$\psi_I = \frac{1}{y_n - y_s} \int_{y_s}^{y_n} \psi_S(x_+(y), y) dy. \tag{9}$$

Therefore the island streamfunction in this idealized setup has a very simple interpretation: it is the average of the Sverdrup streamfunction along the eastern boundary of the island.

The presence of the island circulation changes the standard Stommel-Munk problem. From [6], figure 3 shows an anticyclonic gyre circulation in a circular ocean basin with an island in the center of the tank. The flow is forced by a uniform wind stress curl. The circular basin geometry is different than the rectangle of the original Stommel-Munk problem, which changes the form of the Sverdrup flow and western boundary current. The primary change induced by the island is a recirculation region in the eastern sub-basin. The extent of this recirculation is determined by the latitudes where ψ_I is equal to the Sverdrup flow [6, 5]. The existence of the recirculation is demanded by Kelvin's circulation theorem: southerly flow above and below the recirculation is balanced by a patch of northerly flow in the recirculation. If dissipation $\mathrm{Diss}(\mathbf{u})$ is modeled as bottom friction, the contour integral around the island is conserved: $\oint_C \mathrm{Diss}(\mathbf{u}) \cdot \hat{t} = -r \oint_C \mathbf{u} \cdot \hat{t} = 0$ [6]. This relation requires that the contribution by the western side of the island is negligible.

The Godfrey and Pedlosky et al. island studies above assumed that the island had vertical walls – there is no gradual slope leading from ocean bottom to island top. Assuming vertical walls simplifies the analysis considerably since potential vorticity contours simply follow lines of latitude when there is no bottom topography. Pedlosky et al. (2009) studied the gyre circulation with an island of the form in figure 4. The resulting circulation is shown in figure 5, which can be compared directly to figure 3. The recirculation region has for the most part disappeared. A sharp meander has now formed in the western sub-basin, with streamlines sharply breaking from topographic control to rejoin the southward Sverdrup flow.

3 This report

I will study the above questions – how basin circulation changes when an island is included – but for localized forcing. The above studies mostly concentrated on the case where the surface forcing was basin-wide, the circulation changes considerably when the wind stress curl is localized in space. The remainder of the paper will be organized as follows. Section 4 will describe an unsuccessful attempt to study locally-forced island circulations

in a rotating tank experiment and section 5 will describe more successful numerical models of the circulations.

Numerical model

For the following numerics the model created by Helfrich et al. (1999) was used [2]. The model solves the single layer rotating shallow water equations with bottom friction and viscosity:

$$\begin{aligned}
\frac{\partial u}{\partial t} + u\frac{\partial u}{\partial x} + v\frac{\partial u}{\partial y} - fv &= -g\frac{\partial h}{\partial x} - ru + \frac{\nu}{h}\nabla\cdot(h\nabla u) \\
\frac{\partial v}{\partial t} + u\frac{\partial v}{\partial x} + v\frac{\partial v}{\partial y} - fv &= -g\frac{\partial h}{\partial y} - rv + \frac{\nu}{h}\nabla\cdot(h\nabla v) \\
\frac{\partial h}{\partial t} + \frac{\partial (uh)}{\partial x} + \frac{\partial (vh)}{\partial y} &= 0,
\end{aligned}$$

where h is the fluid height, $f = f_0 + \beta y$ and the second and third terms in the horizontal momentum equations are bottom friction and lateral friction, respectively.

The model was made to mimic the laboratory setup (described below). The model is nondimensionalized using the half width of the basin l as a horizontal length scale, the mean depth H as a vertical length scale, the gravity wave speed $\sqrt{gH}$ as the velocity scale, and the advective time $l/\sqrt{gH}$ as the time scale. A 150x150 grid was used and the model was run out to 6.5 Ekman spindown times, though the model only needed 1-2 spindown times to equilibrate. The model's Stommel layer was resolved by 3 grid widths, the Munk layer by 2 grid widths. This western boundary layer resolution is not ideal, however, the results presented below are reasonable.

3.1 β-plume circulation

The circulation that results from a localized forcing is called a *β-plume* [9, 10, 7]. Figure 6 shows a β-plume circulation in the shallow water model. Unless noted otherwise all wind stress curls are anticyclonic, which induces a southerly Sverdrup flow beneath the forcing. The streamlines roughly follow lines of constant potential vorticity f/H, where H is fluid depth. The edges of the plume expand north and south since the edges of the circulation form small length scales in which friction is important. A zonal boundary layer scaling analysis shows that the plume expands as $\delta_S|x-x_0|)^{1/2}$, where $|x-x_0|$ is the distance from the forcing region located at x_0. Again there is a frictional western boundary current that allows a northward return flow. We will discuss the island results in a later section, but from 9 and the arguments made in section 2 we can already guess that the β-plume cannot

simply use the island to form a western boundary current.

4 The laboratory

The tank used for this experiment is shown from above in figure 7. The tank is square with sides of 60 cm and an average depth of 25 cm. The bottom of the tank is angled with a slope of 0.15 to create a topographic β effect with the top of the picture the effective north. The topographic β equals $f_0 s/H$ where f_0 is the rotation of the tank, s is the bottom slope, and H is the mean depth. An island of length 30 cm is located 23 centimeters east of the western wall. This island has a sloping topographic 'skirt' going from the island surface to the tank bottom. The flow is driven by a stepper motor attached to a rotating disk of radius 7.5 cm located 45 cm east and 30 cm north of the southwest corner (bottom left). There is a rigid lid above the entire flow, with the disk the only moving piece of the lid. The water beneath the rotating lid experiences a constant wind stress curl; this curl drives an Ekman pumping that is balanced by a horizontal geostrophic flow. Diluted food dye was used to visualize the flow, with images taken by a videocamera mounted on the rotating table.

For the rotating table experiment the Munk width $\delta_M = 1.33$ cm and the Stommel width $\delta_S = 0.87$ cm for $f_0 = 2$ s^{-1}. The inertial boundary layer width δ_I can be calculated as $\delta_I = \sqrt{U_S/\beta}$ where $U_S = |w_0|/s$ is the Sverdrup flow driven by a surface Ekman pumping under the disk $w_0 = (\frac{\nu}{\Omega})^{1/2}\Delta\Omega$. ν is the viscosity, $\Omega = f_0/2$ is the rotation of the tank and $\Delta\Omega$ is the differential rotation of the forcing disk.

Figure 7 shows the steady state flow after ninety minutes of spinup. The dye shows up poorly so the flow is highlighted by black arrows. The table rotation was counterclockwise at $f = 2\Omega = 2$ s^{-1} and the disk rotation was clockwise at $Delta\Omega = 0.1$ s^{-1}. The nonlinearity measure $\delta_S/\delta_I = 2.78$, so the flow is being forced strongly. This does not change the conclusions of the following paragraphs, however, and the odd behavior found in the lab was also found for weaker forcings. The dye entry point can be seen along the southeastern side of the island. The red dye does not illuminate any dynamics, so it can be ignored here. Following the arrows in the picture, the blue travels north before it heads east towards the disk. The flow wraps under the disk, then heads back west near the location where the dye was entered. The dye then arcs to the northeast where it wraps *behind* the disk. Once the flow has gone behind the disk it heads west to join back up with the flow to create a recirculation.

A northward flow to the *east* of the forcing region is a problem since the tank is a rigid lid

system with negligible buoyancy effects. The only method of communicating information in the system is Rossby waves propagating on the topographic β. Since $\beta > 0$ the Rossby waves propagate to the west and consequently a water parcel to the east of the forcing region has no way of knowing that there is any forcing, and thus should not be moving.

The first guess as to what was going wrong was something involving the imperfect laboratory setup: unaccounted for buoyancy effects, incorrect rotation–either from the table itself or from placement on the table, or incorrect forcing. These are issues that do not effect the shallow water model, so we next tried to emulate the laboratory flow in the model.

The result is shown in figure 8. A clockwise rotating circulation emanates from the disk and heads towards the island, returning after heading north on a frictional boundary layer. A counter-clockwise rotating circulation can be seen behind the clockwise circulation, very much as in the laboratory experiment. Therefore the problem is not with the laboratory, but with the setup. The laboratory forcing did not turn out as intended.

In the laboratory experiment the azimuthal surface stress is as follows

$$\tau(r) = \begin{cases} \tau_{\max} r/R & : r \leq R \\ 0 & : r > R \end{cases}$$

where $\tau_{\max}$ is the maximum stress and r is the radial distance from the disk center. The curl of the stress is

$$\mathrm{curl}\tau(r) = \begin{cases} 2\tau_{\max}/R & : r \leq R \\ -\mathrm{sgn}(\tau_{max})\delta(r-R) & : r = R \\ 0 & : r > R \end{cases}$$

since the there is a discontinuous jump in stress from $r = R$ to $r > R$. This oppositely signed ring of stress curl drives the counter-rotating flow that shows up just to the east of the forcing. Friction causes the circulation to spread in the laboratory; in the model this discontinuity in curl is spread over a grid cell.

This problem was corrected in the model by changing the stress term outside the disk to

$$\tau(r) = \begin{cases} \tau_{\max} r/R & : r \leq R \\ \tau_{\max} R/r & : r > R \end{cases}$$

This gives zero curl outside the disk. The nonzero stress for $r > R$ does generate a small Ekman transport, but this has a negligible effect on the flow for weak forcing. For the remainder of this report I will discuss numerical model runs forced with this corrected stress distribution.

5 Numerics

5.1 Vertically-walled island

A vertically walled island is now included in the basin. The island is one nondimensional unit long in y centered at $y = 0.7$. The island is two grid cells in width as required by the numerics. The circulation is shown in figure 9. The center of the β-plume is interrupted on its way west and a recirculation region the width of the forcing region extends to the island. The outer edges of the plume continue west until intersecting the western side of the domain, forming a boundary layer. The island intersection of these two parts of the β-plume determine stagnation points of the circulation at $y \approx 0.7, 1.3$ along the eastern side of the island.

This flow satisfies the island rule (**??**) and the structure of the eastern sub-basin circulation is analogous to the circulation on the eastern side of the vertically walled island in figure 3 (Pedlosky et al. (1997)). The recirculation region in figure 9 is a stretched out form of the recirculation in figure 3. Moving south to north along the eastern side of the island in both circulations the velocity changes from southward to northward to southward, again satisfying the circulation constraint $\oint_C \mathrm{Diss}(\mathbf{u}) \cdot \hat{t} = -r \oint_C \mathbf{u} \cdot \hat{t} = 0$, again assuming that the primary dissipative process is bottom friction $\mathrm{Diss}(\mathbf{u}) = -r\mathbf{u}$ acting on the eastern side of the island.

The same considerations apply when the basin geometry is varied. When the island is small relative to the forcing the circulation looks like a β-plume with slightly modified contours where the island lies (figure 10). When the island is large relative to the forcing the western basin response is the scale of the island (figure 11). These two figures show that the size western basin response will scale as the larger of the island and forcing meridional lengthscales. This still holds if the forcing region is moved relative to the island. In figure 12 the forcing is moved to the south but since a piece of the β-plume hits the island the western sub-basin response is the size of the island.

5.2 Island with topography

The topographic island placed in the basin is shown in figure 13. The shallow water model used for these numerics becomes unstable when the island reaches to the surface so the island was only made to reach 3/4 of the way to the surface. The dynamics of the 'submerged' island are assumed to be very similar to an island reaching to the fluid top since there are closed f/H contours surrounding the (submerged) island. The submerged island could also be thought of as a seamount.

Adding a topographic island changes the geometry of potential vorticity f/H contours. In the absence of friction a linear flow will follow f/H contours. A topographic island is very different from a vertically-walled island because topography creates closed f/H contours, whereas the vertical island merely disrupts f/H contours, exactly like the eastern and western boundary in the Stommel or Munk problem. We might expect the flow to look like the sketch in figure 14, with the flow only leaving an f/H contour when encountering the western boundary. This however, is not what happens, and the the resulting circulation is shown in figure 15 for a case with $\delta_I/\delta_S = 0.33$

The circulation has changed drastically compared to the vertically walled island in figure 9. There is still a main recirculation region, but it now reaches all the way to the southwestern tip of the island. The topography has a strong control on the flow, with the streamfunction lines for the most part tracking f/H contours, except in small areas where friction is important. The around island flow also differs from the vertically-walled case. As the return flow comes around the northern edge of the island it tracks south on a f/H contour, but then takes a hard left turn and heads *north* towards the forcing region. This sharp meander is reminiscent of the meander in figure 5 from Pedlosky et al. (2009). In the Pedlosky et al. paper the meander is in the western sub basin – in the localized forcing case in figure 15 the meander is to the east of the island. The meander again allows the circulation to satisfy the circulation constraint, the return flow of the main recirculation cell moves *counterclockwise* (mostly northward) with respect to a closed f/H contour, while the flow returning from the western sub-basin moves *clockwise* (mostly southward). The reason that the flow does not follow the course shown in figure 14 is friction: there is enough friction for the flow to 'slide' off of f/h contours and travel all the way around the island. In fact the main recirculation region is simply a truncated version of the sketch in figure 14, with the flow only making it to the southern tip of the island before it gets rerouted from its course to the western wall.

With cyclonic forcing the circulation response is the same, but with opposite sign, as expected for the linear regime.

5.3 Increasing non-linearity

The numerical model used was designed to study inertial flows and was not ideal for this problem. Thus we were not able to study the entire range of parameter space that we would have liked. For example it was difficult to modify lateral and bottom friction and change the geometry of the sloped island. However we were able to get interesting results for changing δ_I/δ_S, the nonlinearity factor, by increasing the strength of the wind stress curl. Results for both anticyclonic and cyclonic forcing are shown in figures 16(a)-16(d). Increasing the nonlinearity pushes the center of the western boundary current to the north (south) corner for anticyclonic (cyclonic) forcing. The main recirculation region becomes deformed and stretches to the south. For $\delta_I/\delta_S = 7.37$ with a vertically-walled island the flow is unsteady, with vortices being shed off the southern tip of the island (not shown). This unsteadiness, which was not found in the topographic island circulation, may be a result of flow separation at the sharp corners of the vertically walled island.

6 Conclusions

The presence of an island in a basin with localized wind stress curl significantly changes the standard β-plume response. Whether the island has vertical walls or a topographic slope the circulation is split into two components. The bulk of the circulation stays close to the eastern side of the island, forming a small recirculation region that includes most of the forcing area. In the vertically walled case, this recirculation forms a rectangular region with latitudinal scale defined by the size of the forcing region. In the topographic slope case the western side of the main recirculation region is diffused southward, with a small component of the flow reaching the southwestern tip of the island topography. The second component of the flow travels around the island, using the western edge of the basin to form a western boundary current. This flow is for the most part quite similar for both islands – the circulation acts as an interrupted β-plume, extending around the southern and northern edges of the island. This around-island flow does differ significantly on the return by the northern edge of the island. In the topographic case, the return flow tracks almost due south along an f/H contour until sharply jumping north to rejoin the forcing region and forming a meander. All of the around-island dynamics appear for the most part to be governed by Kelvin's circulation theorem about the island: $\oint_C \mathrm{Diss}(\mathbf{u}) \cdot \hat{t} \approx -r \oint_C \mathbf{u} \cdot \hat{t} = 0$. Thus around the island, or in the topographic case around a closed f/H contour about the island, the clockwise flow must balance the counterclockwise flow. In the vertically walled case this requirement creates a recirculation zone analagous to that found in Pedlosky et al. (1997) and in the topographic case it creates a sharp meander in the eastern sub-basin.

An interesting effect of the island is that even when the forcing radius is very small relative to the island length the circulation response *must* be on the scale of the island. This is again due to the circulation constraint on a closed contour of the flow about the island and the act of friction forcing flow off of f/H contours. This dramatic effect of the island on the basin circulation is not seen in the studies with basin-wide forcing.

6.1 Future Work

It is easy to change the relative size, shape, and relative position of the forcing region and island within the model. The results found in this study and some results not placed in this report suggest that the bulk of the possible flow types are captured well by the two examples given above. However there are many basin and forcing geometries and some may give fundamentally different circulations. Related to this, it would be nice to replicate the numerical results in this paper with a model more suited to slow, linear ocean circulations. The model used here was created to study inertial flows and worked quite well but was not perfect: it was not amenable to turning off lateral friction or turning down bottom friction, and had issues with some island geometries. Lastly, to study this problem in the lab would require a mass source-sink setup that was either a point source or a source over a general area that induced an Ekman pumping directly. It would be interesting to see if the lab results match up with the numerical results over a wide range of forcings.

References

[1] J. S. Godfrey, *A sverdrup model of the depth-integrated flow for the world ocean allowing for island circulations*, Geophysical and Astrophysical Fluid Dynamics, 45 (1989), pp. 89–112.

[2] K. Helfrich, A. C. Kuo, and L. Prattl, *Nonlinear rossby adjustment in a channel*, J. Fluid Mech., 390.

[3] W. H. Munk, *On the Wind-Driven Ocean Circulation.*, Journal of Atmospheric Sciences, 7 (1950), pp. 80–93.

[4] J. Pedlosky, *Ocean circulation theory*, Springer, 1996.

[5] J. Pedlosky, R. Iacono, E. Napolitano, and K. Helfrich, *The skirted island: The effect of topography on the flow around planetary scale islands*, Journal of Marine Research, 67 (2009), pp. 435–478.

[6] J. Pedlosky, L. J. Pratt, M. A. Spall, and K. R. Helfrich, *Circulation around islands and ridges*, Journal of Marine Research, 55 (1997), pp. 1199–1251.

[7] M. Spall, *Buoyancy-forced circulations around islands and ridges*, Journal of Marine Research, 58 (2000), pp. 957–982.

[8] H. Stommel, *The westward intensification of wind-driven ocean currents*, Trans. Amer. Geophys. Union, 99 (1948), pp. 202–206.

[9] H. Stommel, *Is the south pacific helium-3 plume dynamically active?*, Earth and Planetary Science Letters, 61 (1982), pp. 63 – 67.

[10] G. K. Vallis, *Atmospheric and Oceanic Fluid Dynamics*, Cambridge University Press, Nov. 2006.

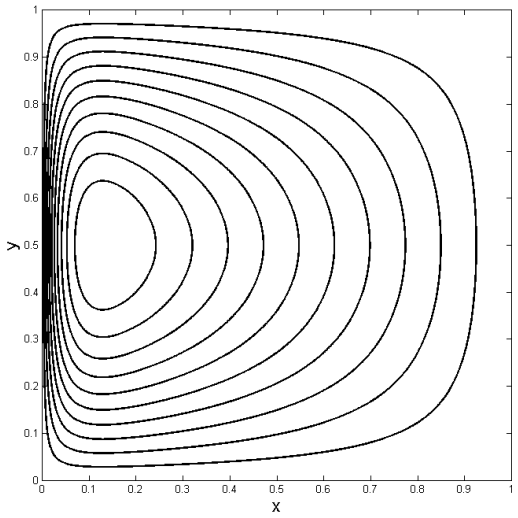

Figure 1: Following [10], the solution streamfunction of the Stommel problem with $d = 0.04$.

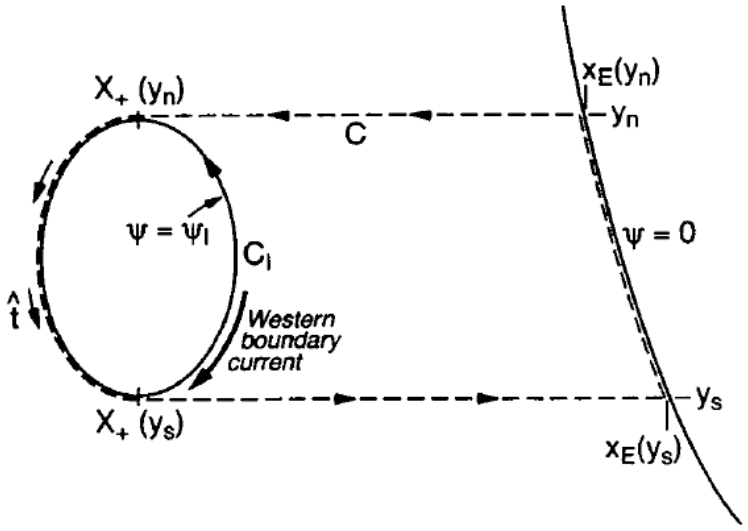

Figure 2: The contour integral allowing for the evaluation of the island circulation, from [6].

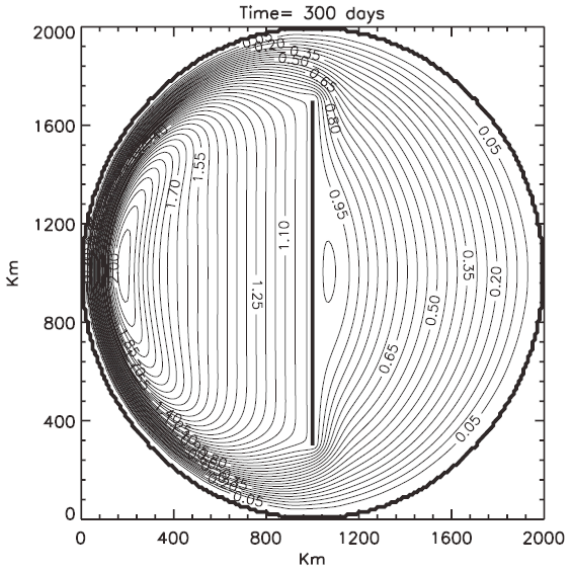

Figure 3: Linear gyre circulation in a circular basin with a vertically-walled island [5]. The forcing is anticyclonic. The island is represented by the bar in the center of the basin.

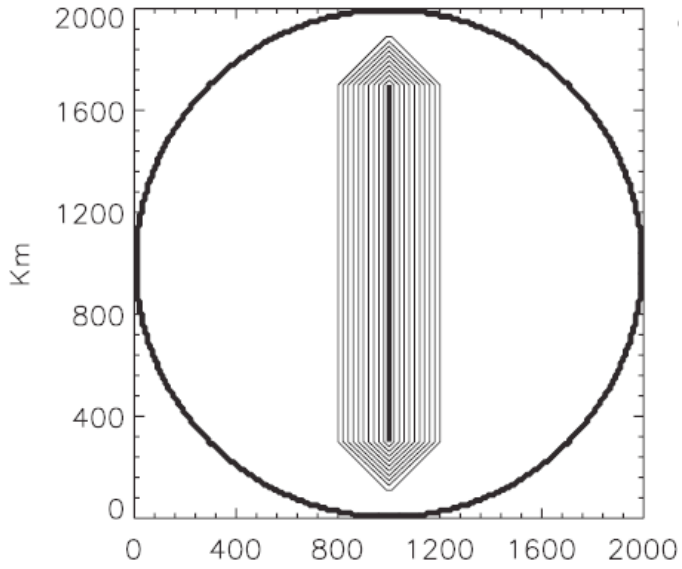

Figure 4: The island with topography from [5].

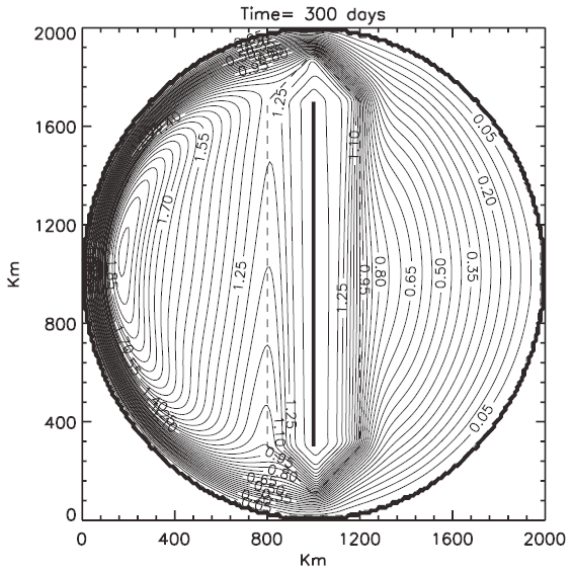

Figure 5: The circulation in a gyre with the island from figure 4(from [5]). The dashed line marks the outer edge of the island topography.

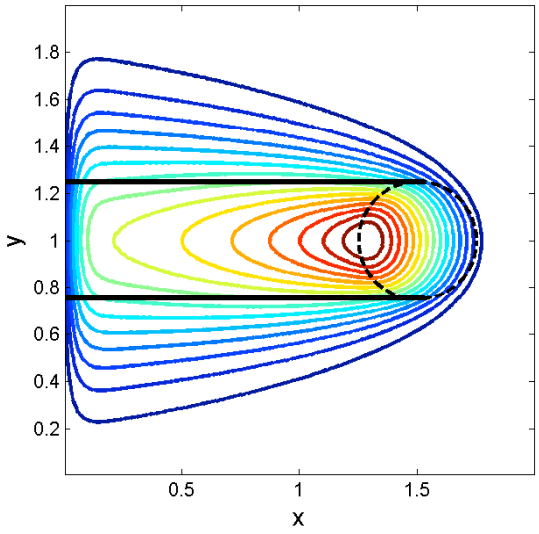

Figure 6: A β-plume circulation forced by a disk of constant wind stress curl centered at $(x, y) = (1.5, 1)$ with radius 0.25. The straight black lines indicate the width the beta plume would have if there were no friction. $\delta_I/\delta_S = 0.33$.

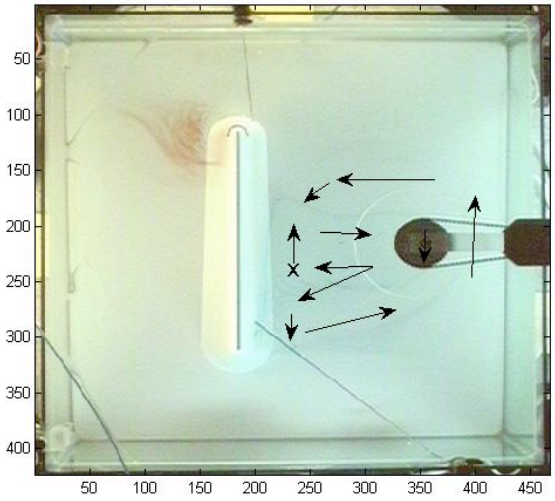

Figure 7: A run of the rotating table experiment. Starting at **X** the arrows denote the path of a water parcel through the flow.

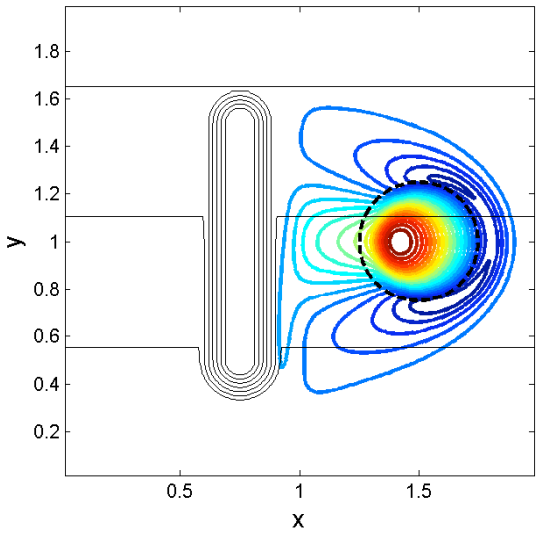

Figure 8: Steady state streamfunction from the numerical model in a setup mimicking the laboratory experiment. Black lines denote height contours.

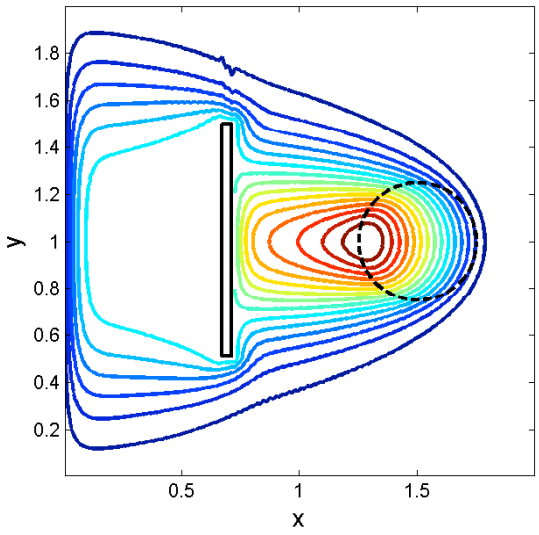

Figure 9: Circulation with a vertically walled island. $\delta_I/\delta_S = 0.33$.

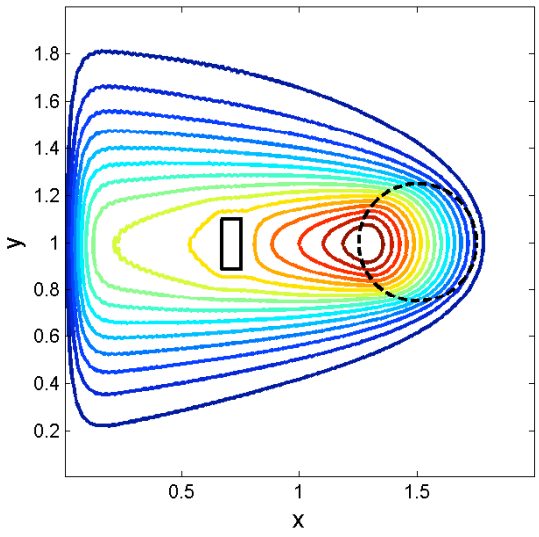

Figure 10: Circulation with a vertically walled island with length 0.2. $\delta_I/\delta_S = 0.33$.

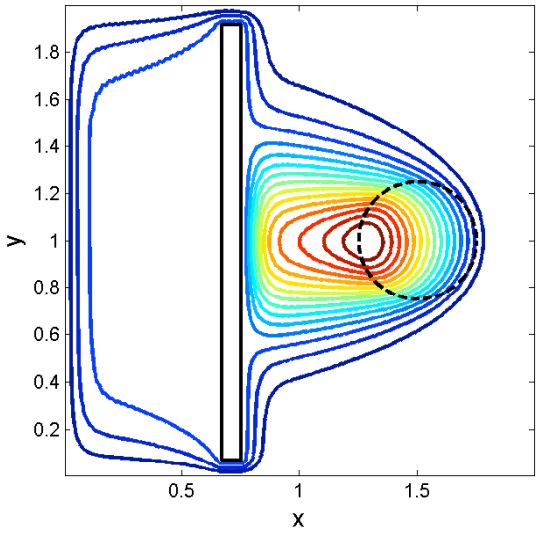

Figure 11: Circulation with a vertically walled island with length 1.95. $\delta_I/\delta_S = 0.33$.

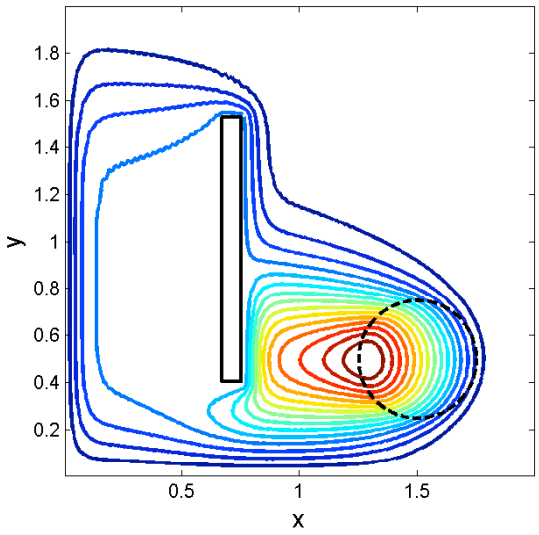

Figure 12: Circulation with a vertically walled island and the forcing centered at $(x, y) = (1.5, 0.5)$. $\delta_I/\delta_S = 0.33$.

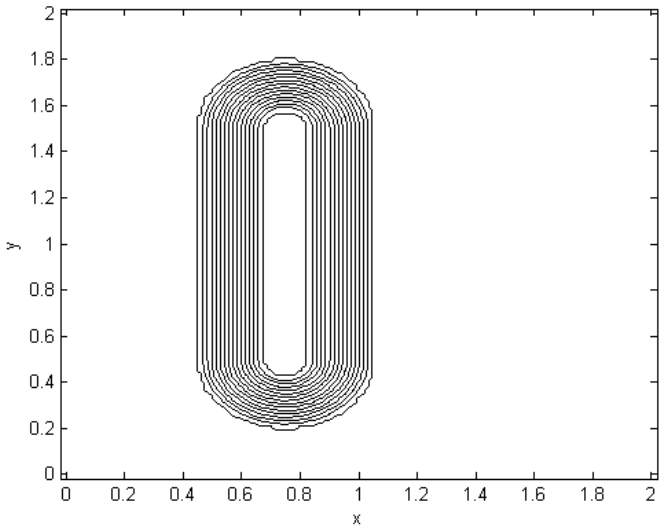

Figure 13: Height contours of the topographic island. Contours are spaced 0.05 nondimensional units apart to a maximum of 0.75. The total height of the fluid is 1.

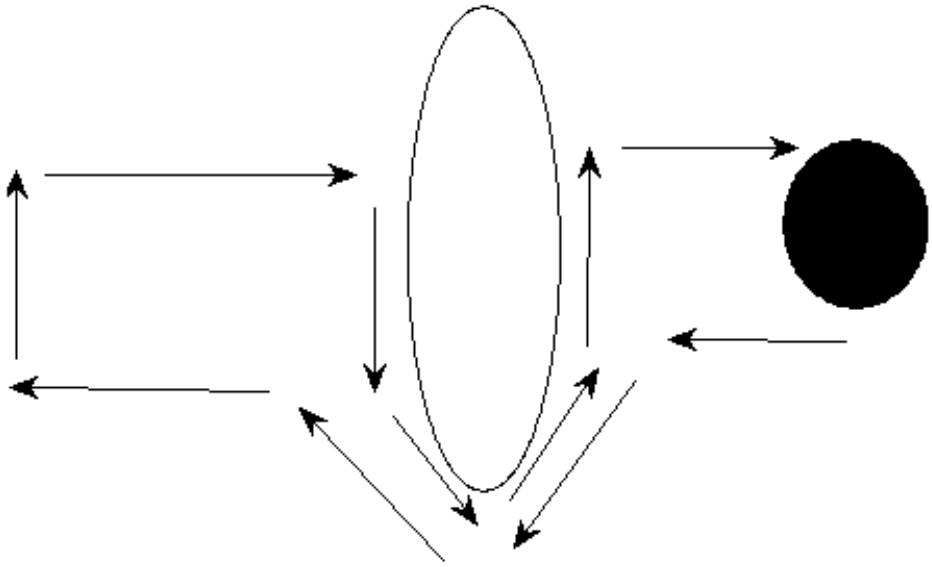

Figure 14: A sketch of the expected flow in a basin with a topographic island. The open figure is the outermost closed f/H contour defined by the island, the closed figure is the forcing region.

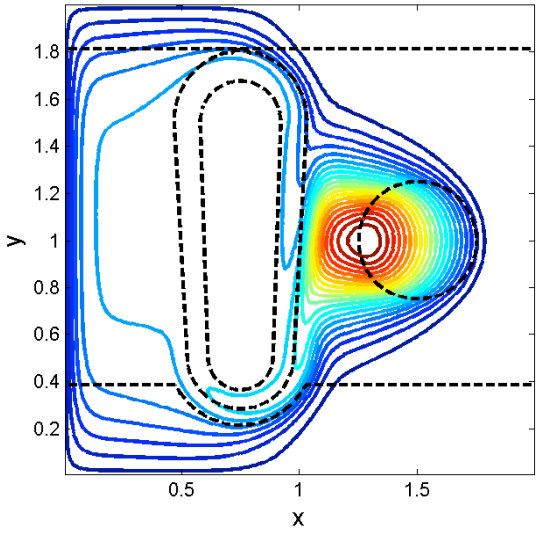

Figure 15: Circulation in a basin with the topographic island from figure 13. Black contours denote potential vorticity f/H. The largest closed contour is the potential vorticity contour enclosing the island. $\delta_I/\delta_S = 0.33$.

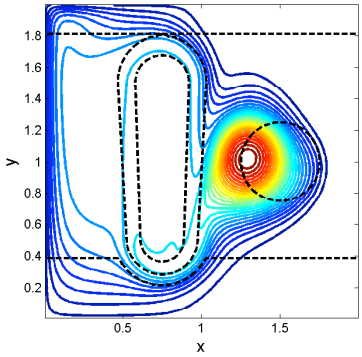

(a) Circulation for topographic island with anti-cyclonic forcing and $\delta_I/\delta_S = 3.30$.

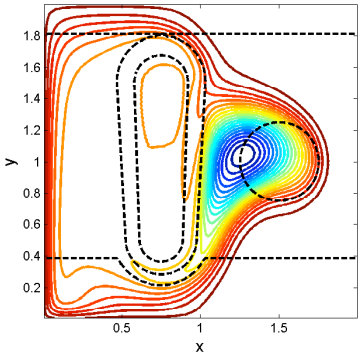

(b) Circulation for topographic island with cyclonic forcing and $\delta_I/\delta_S = 3.30$.

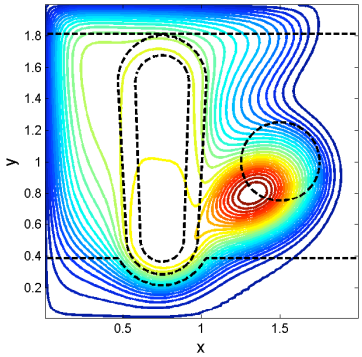

(c) Circulation for topographic island with anti-cyclonic forcing and $\delta_I/\delta_S = 7.37$.

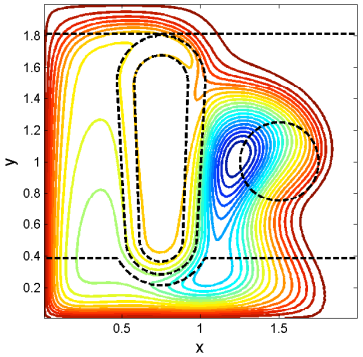

(d) Circulation for topographic island with cyclonic forcing and $\delta_I/\delta_S = 7.37$.

Figure 16: Circulations for increasing non-linearity.